A study of structural and chemical properties of $Ni_{1-x}Zn_xFe_2O_4$ ferrite powder prepared by co-precipitation method

R. R. Ahmed[a,*], T. H. Mubarak[a], I. H. Mohamed[b]
[a]*Department of Physics, College of Science, University of Diyala, Diyala, Iraq*
[b]*Department of Biology, College of Science, University of Diyala, Diyala, Iraq*

Nickel zinc nanoferrites ($Ni_{1-x}Zn_xFe_2O_4$ with x ranging from 0.3 to 0.7 and 0.9) were employed in this study. Chemical co-precipitation was used to synthesize nanoparticles, X-ray diffraction, fourier transform infrared spectroscopy, field emission scanning electron microscopy analysis (FESEM), and the vibration sample magnetometer were used to determine the structure, size, morphology, and magnetic properties of nanostructures (VSM). X-ray diffraction was used to identify the crystalline phases, and all samples have cubic spinel ferrites. To evaluate particle sizes using Scherrer's formula. average crystallite sizes were in the range of (13-19)nm and FTIR spectroscopy data for respective sites were examined in the range of 200–4000 cm^{-1} . Between 320 and 1000 cm^{-1}, the formation of ferrite phase was confirmed, indicating the sample's ferrite nature. Tetrahedral complexes were assigned to the higher frequency band ν_1, while octahedral complexes were assigned to the lower frequency band ν_2. The M-H curve shows that Ms rises from 1.96-23.7 (emu/g).

1. Introduction

In recent years, nanocrystalline magnetic materials have piqued researchers' interest because of their large number of novel physical properties [1].The quantum size effect, combined with the large surface area of magnetic nanoparticles, dramatically alters some magnetic properties and causes superparamagnetic phenomena. Spinel ferrites nanocrystals were synthesized with the goal of creating a better material with excellent chemical stability, low magnetic coercivity, moderate saturation magnetization, and high permeability at room temperature [2, 3]. Nanomaterials outperform bulk materials in terms of structural, electrical, and magnetic properties. Because of its improved structural and magnetic properties, magnetic nonmaterial becomes a promising candidate in a variety of applications such as gas sensors, magnetic hyperthermia, drug delivery, memories storage, and so on [4-6].Depending upon the crystal structure, ferrites are classified into three categories: spinel ferrite, garnet ferrite and hexagonal ferrite. MFe_2O_4 is the general spinel ferrite formula, where M is a divalent metal ion like Ni^{2+},Zn^{2+}, Co^{2+}, Mn^{2+}, etc.[7].

The divalent cations, which occupy the tetrahedral A sites, and the trivalent cation, which has a high degree of affinity for the octahedral B sites, control the magnetic properties of ferrites in the AB_2O_4 spinel structural formula [8, 9]. Zn ferrite bulk material has a normal spinel structure, with all divalent cations on the tetrahedral sites and all trivalent cations on the octahedral sites. In contrast, Ni ferrites bulk materials have an inverse spinel structure, with half of trivalent cations occupying tetrahedral sites and the other half remaining on octahedral, and divalent cations all migrating to octahedral positions. It has been shown that octahedral sites prefer Ni and tetrahedral sites prefer Zn in Ni-Zn ferrite nanoparticles [10].The $Ni_{1-x}Zn_xFe_2O_4$ nanoparticles are synthesized by numerous techniques such as solgel [11], citrate precursor route [12], co-precipitation [13, 14], thermal composition method [15], micro-emulsion [16] and sonochemical reaction [17]. Some disadvantages of these methods include a complicated procedure, a high reaction temperature, a long reaction time, and the use of reduction agents, all of which have the potential to pollute the environment.

In the present work, synthesis of $Ni_{1-x}Zn_xFe_2O_4$ nanoferrites was carried out by chemical co-precipitation method because it is a simple, cost-effective method that does not require any organic fuel. Low temperature, small particle size, high porosity, short time of preparation, high purity, strong chemical homogeneity, crystallinity and a simple process, are some of the great benefits of the co-precipitation process. In comparison to other methods, the co-precipitation method is better for synthesis of required sized nanoparticles, according to L.C. Sonia et al [15]. The structural, morphological, and magnetic properties of Ni substituted Zn ferrite synthesized by chemical co-precipitation are investigated in this paper.

2. Experiments and measurements

2.1. Preparation of nanomaterials

All of the materials were analytically graded and were utilized without further purification after purchase. Starting components include sources of ferric chloride, Nicle chloride $NiCl_2$, zinc chloride $ZnCl_2$ and sodium Hydroxide NaOH. The co-precipitation method was used to make $Ni_{1-x}Zn_xFe_2O_4$ nanoferrites, which were then used to make Nickel zinc ferrite nanoparticles. A 1:2 molar ratio of $NiZnCl_2$ and $FeCl_3$ was dissolved in distilled water with constant stirring to make the solution. 5g of NaOH dissolved in (100 ml) was added drop by drop with constant stirring. The pH of the solution was maintained at 12 during precipitation, and dark grey precipitates were obtained after adding NaOH. The mixture was then heated at 90 C for 1h to obtain the precipitated particles. These precipitated particles were then washed several times with distilled water to remove the salt residues and other impurities. Finally, the powder samples were calcined at 700^0C for 3h.

2.2. Characterization

The crystalline phases calcined samples at 700 ^{0}C and were identified by x-ray diffraction (Phillips Xpert, Holland) with CuKα radiation (λ = 1.5418 A), operated at 30 mA current and 40 kV voltage in the 2θ range from 20° to 80°. FT-IR spectra were recorded for prepared nanoparticles with a Shimazdu FTIR spectrometer at room temperature within the wavenumber range 200cm^{-1} - 4000 cm^{-1} and transmittance spectrum was obtained. The morphology of powders were examined by field emission scanning electron microscope (FESEM, Model Sigma VP,Zeiss, Germany). The magnetic properties of the ferrites were measured using a vibrating sample magnetometer (VSM; LBKFB model Meghnatis Daghigh Kavir Company) at room temperature in a maximum applied field of 20 kOe. In addition, the saturation magnetization (Ms), the remanence magnetization (Mr) and the coercivity (Hc) were determined by the obtained hysteresis loops.

3. Results and discussion

3.1. XRD studies

Figure 1 shows the XRD patterns for $Ni_{1-x}Zn_xFe_2O_4$ nanoferrites at different zinc ratios (x) varied from 0.3, 0.7 and 0.9 calcined at 700°C for 3 h. The diffraction peaks corresponding to (220), (311), (222), (400), (422), (511), (440) and (533) planes of Ni-Zn ferrite perfectly agreed with the theoretical data of the $Ni_{1-x}Zn_xFe_2O_4$ spinel structure (ICSD cards No. 01-070-6496). The XRD patterns confirm that all the samples exhibit a polycrystalline FCC spinel structure. The full width at half maximum of the strongest reflection was used to calculate the crystallite sizes using Scherrer equation [18-20] as mentioned below.

$$D = \frac{K\lambda}{\beta \cos\theta} \tag{1}$$

Here, D represents the crystallite size, β is the full width at half maximum (FWHM) of the (3 1 1) peak in radian, K is the shape function equivalent to 0.9, λ is the X-ray wavelength, and θ is the diffraction angle. We synthesized all $Ni_{1-x}Zn_xFe_2O_4$ nanoferrites under similar conditions,

though the crystallite size for zinc concentration was not the same, perhaps due to preparation circumstances, that resulted in different ferrite formation rates. The values of lattice constant and crystallite size are shown in Table 1. The lattice constant (a) of nickel zinc nanoferrites increases from 8.33 Å to 8.42 Å with an increase in zinc content in Ni-based ferrites. According to Gul et al [21, 22], Zn^{2+} have larger ionic radius (0.83 Å) than Ni^{2+} (0.74 Å) and Fe^{3+} (0.65 Å) ions. There is a uniform increment in lattice constant with Zn substitution, which emonstrates that the lattice grows without deteriorating the lattice symmetry of the lattice [23].
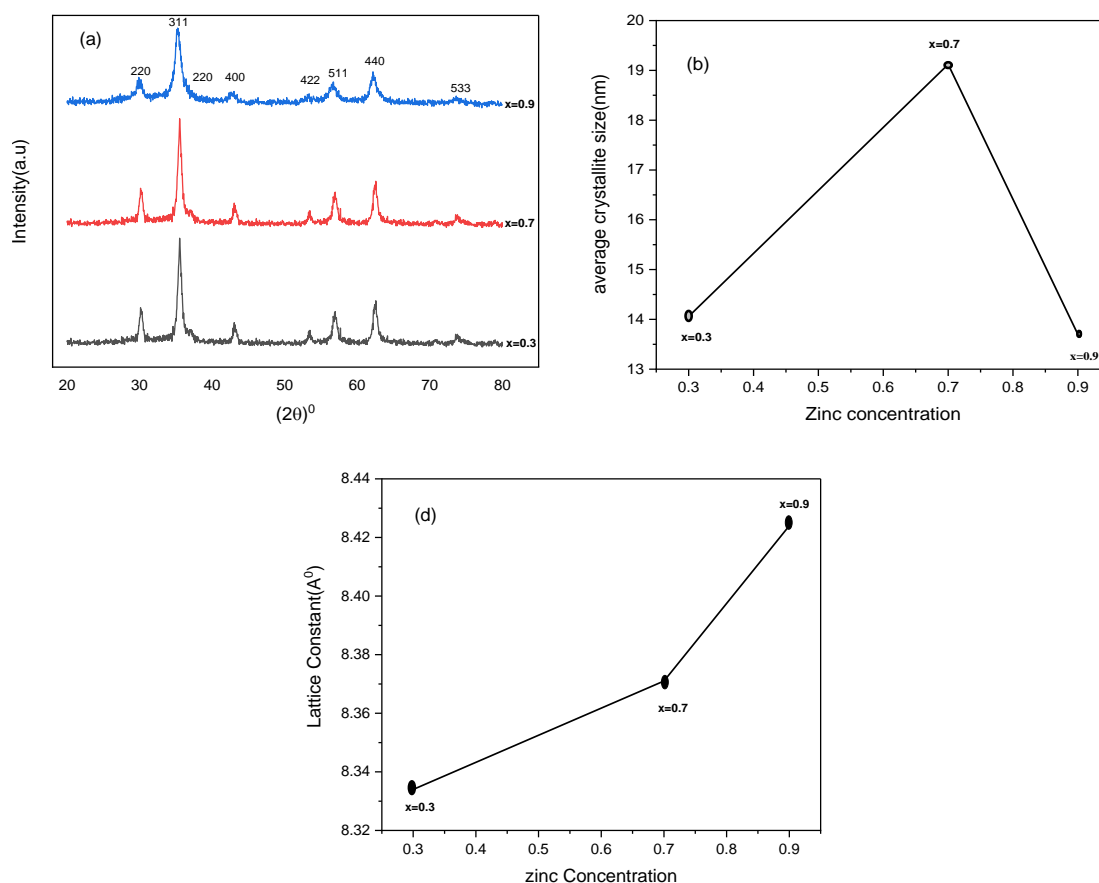

Fig. 1. (a) The X-Ray diffraction pattern for $Ni_{1-x}Zn_xFe_2O_4$ nanoferrites (x = 0.3, 0.7, 0.9).
The influence of Zn concentration on average (b) crystallite size, (d) lattice constant.

Table 1. Structural parameters of $Ni_{1-x}Zn_xFe_2O_4$ nanoparticles.

Molar ratio	Molar ratio	Composition	2θ	a(Å)	dx(g/cm^3)	D(nm)
N1	0.3	$Ni_{0.7}Zn_{0.3}Fe_2O_4$	35.687	8.334	12.2	14.06
N2	0.7	$Ni_{0.3}Zn_{0.7}Fe_2O_4$	35.536	8.371	12.1	19.12
N3	0.9	$Ni_{0.1}Zn_{0.9}Fe_2O_4$	35.295	8.424	11.8	13.7

3.2. FT-IR Spectroscopy analysis

Figure 2 shows the spinel structure caused by foreign ions or the cationic distribution of $Ni_{1-x}Zn_xFe_2O_4$ with x=0.3,0.7, and 0.9. Also, Table 2 summarizes the main transmittance frequencies observed in the region 200–4000 cm^{-1} of the FTIR spectra for $Ni_{1-x}Zn_xFe_2O_4$ nanoferrites with x varying. All the samples display pure spinel phase in the wavelength range of 320–1000 nm. The frequency band at a higher wavelength v_1 (555.49–572.85cm^{-1}) is due to the presence of tetrahedral complexes, while the lower frequency bands v_2 (374.19-385.76) illustrates

the octahedral complexes. The FTIR analysis shows that the normal vibrational mode of a tetrahedral cluster is greater in comparison with the octahedral cluster. The reason is that the octahedral group possesses longer bond length, while the tetrahedral cluster has a shorter bond length. According to the geometric configuration of ferrites, the metal cations were located nearest to oxygen ions, in two different sublattices of ferrites, namely tetrahedral (A-sites) and octahedral (B-sites) [24]. The band located at $3487 cm^{-1}$ could be attributed to the symmetric vibration of –OH groups. The peak at $2366 cm^{-1}$ was ascribed to H-O-H bending vibration of the free or absorbed water[25]The band position differences (ν_1 and ν_2) arise due to difference in the $Fe^{+3}-O^{-2}$ distance for tetrahedral and octahedral complexes [26]. Generally, the vibrational frequency is dependent on cation mass, bonding force, and cation–oxygen distance [27].
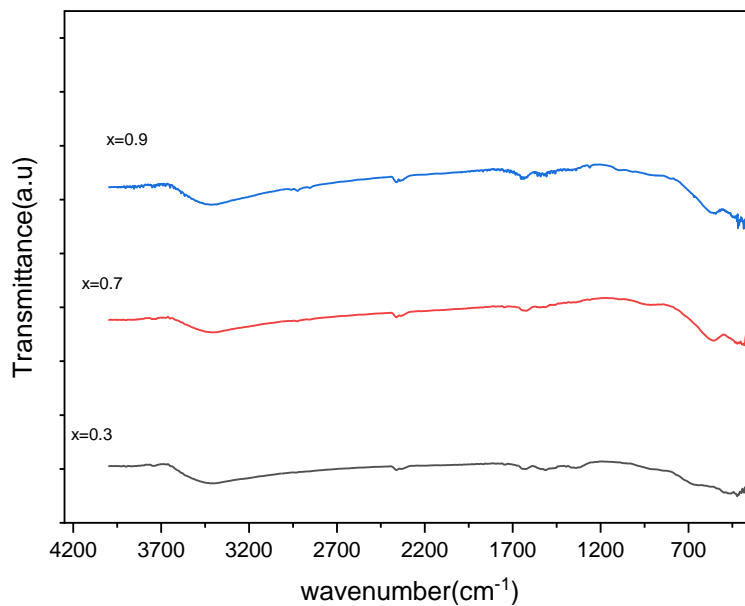

Fig. 2. FTIR spectra of $Ni_{1-x}Zn_xFe_2O_4$ nanoferrites (x = 0.3,0.7 and 0.9).

Table 2. Vibrational frequencies corresponding to tetrahedral and octahedral metal of $Ni_{1-x}Zn_xFe_2O_4$ nanoferrites.

samples	Molar ratio	composition	$\upsilon_{T(cm^{-1})}$	$\upsilon_{B(cm^{-1})}$
N1	0.3	$Ni_{0.7}Zn_{0.3}Fe_2O_4$	555.49	374.19
N2	0.7	$Ni_{0.3}Zn_{0.7}Fe_2O_4$	582.5	381.9
N3	0.9	$Ni_{0.1}Zn_{0.9}Fe_2O_4$	572.85	374.19

3.3. FE-SEM of $Ni_{1-x}Zn_xFe_2O_4$ nanoferrite

A high-resolution field emission scanning electron microscope (FE-SEM) operating at 10.00 KV was used to examine the morphology of $Ni_{1-x}Zn_xFe_2O_4$ nanoferrites samples with various compositions. We used powder samples for the morphological analysis. All of the samples have a spherical shape and a narrow size range. It is observed that the particle uniformity, few clusters and agglomeration of ferrite nanoparticles Figure. 3 due to its magnetic nature and the union of primary particles held together by weak surface interaction such as the van der Waals forces between the particles indicated [28]. The particle size of the synthesized samples lies in the nanometer scales 30–60 nm.
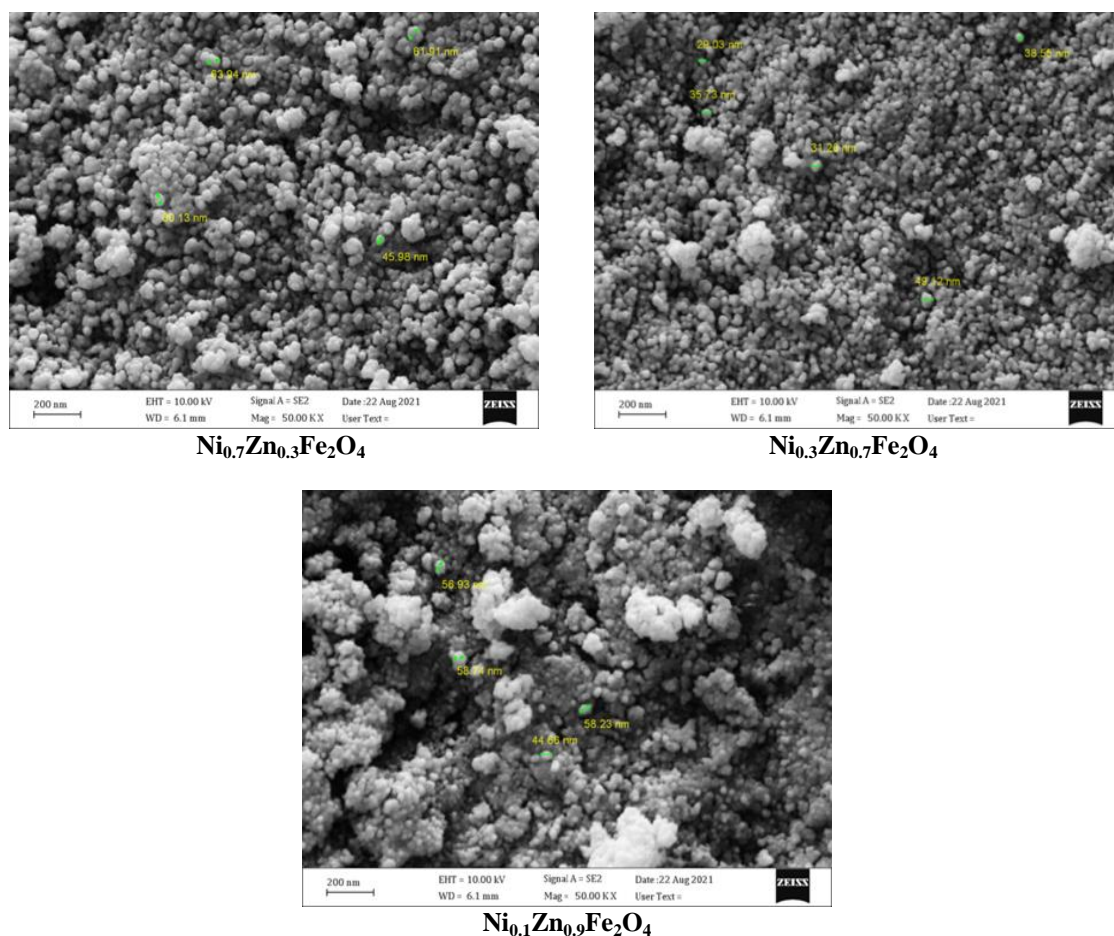
Ni$_{0.7}$Zn$_{0.3}$Fe$_2$O$_4$ **Ni$_{0.3}$Zn$_{0.7}$Fe$_2$O$_4$**

Ni$_{0.1}$Zn$_{0.9}$Fe$_2$O$_4$

Fig. 3. The FESEM analysis for Ni$_{1-x}$Zn$_x$Fe$_2$O$_4$ (x = 0.3, 0.7, 0.9) nanoparticles with increasing zinc concentration.

3.4. Magnetic measurements

The magnetic behavior of Ni$_{1-x}$Zn$_x$Fe$_2$O$_4$ nanoparticles investigated using VSM is shown in Figure 4. The lower saturation magnetization value (1.96 and 5.79 emu/g)for nanoparticles may be due to lattice defects, larger surface areas, and thus high surface energy and surface tension, resulting in random spin orientation on the surface of nanoparticles [29, 30]. The remanence magnitude (Mr), can be calculated by intersecting the hysteresis loop with the vertical magnetization axis. Table .5 depicts the values of saturation magnetization (Ms), remanence magnitude (Mr) and coercivity (Hc) of different samples. The coercivity for a ferromagnet or ferrimagnet can be reflected by the coercivity field (Hc). This value refers to the intensity of the magnetic field required to reduce the magnetization of the magnetic sample to zero, after the magnetization of the sample has reached saturation[31].
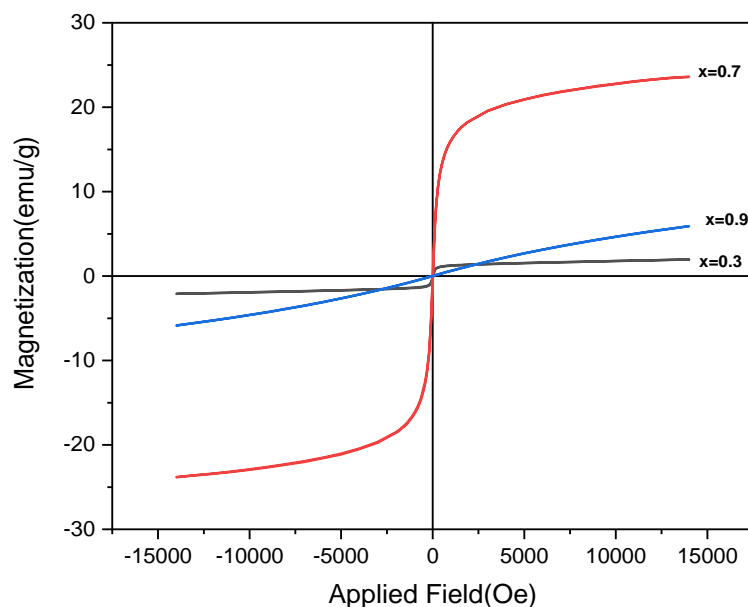
Fig. 4. Hysteresis loops of $Ni_{1-x}Zn_xFe_2O_4$ nanoferrite.

Table 3. Magnetic properties variation of $Ni_{1-x}Zn_xFe_2O_4$ nanoferrite.

Molar ratio	sample	MS(emu/g)	Hc(Oe)	Mr(emu/g)	S=Mr/Ms
0	$Ni_{0.7}Zn_{0.3}Fe_2O_4$	1.96	0.0055	0.082	0.041
0.3	$Ni_{0.3}Zn_{0.7}Fe_2O_4$	23.7	0.013	0.066	0.0027
0.9	$Ni_{0.1}Zn_{0.9}Fe_2O_4$	6.81	0.002	0.024	0.0035

4. Conclusions

The co-precipitation method was used to make $NiZnFe_2O_4$ nanoferrites, which was thoroughly discussed in the paper. The cubic spinel structure was observed in the XRD pattern, with very small particle sizes. The formation of ferrite phase was confirmed by the two absorption bands occurred between 320 cm^{-1} and 590 cm^{-1} characterizing the ferrite nature of the sample. The FESEM analysis confirmed and demonstrated that the nanoparticles agglomerated to form spherical-shaped particles, and the saturation magnetization revealed the superparamagnetic nature of the sample for x=0.3 and x=0.9, whereas the material is ferromagnetic for x=0.7.

References

[1] M. Zheng, X. Wu, B. Zou, Y. Wang, Journal of magnetism and magnetic materials, vol. 183, no. 1-2, pp. 152-156, 1998; https://doi.org/10.1016/S0304-8853(97)01057-3

[2] A. Mohammad, S. Aliridha, T. Mubarak, Digest Journal of Nanomaterials & Biostructures (DJNB), vol. 13, no. 3, 2018.

[3] M. B. Jumaa, T. H. Mubarak, A. M. Mohammad, Synthesis, vol. 15, no. 2, pp. 74-82, 2021.

[4] C. Murugan, V. Sharma, R. K. Murugan, G. Malaimegu, A. Sundaramurthy, Journal of Controlled Release, vol. 299, pp. 1-20, 2019; https://doi.org/10.1016/j.jconrel.2019.02.015

[5] S. R. Patade, D. D. Andhare, S. B. Somvanshi, P. B. Kharat, S. D. More, K. M. Jadhav, Nanomaterials and Energy, vol. 9, no. 1, pp. 8-13, 2020; https://doi.org/10.1680/jnaen.19.00006

[6] S. B. Somvanshi, S. R. Patade, D. D. Andhare, S. A. Jadhav, M. V. Khedkar, P. B. Kharat, P. P. Khirade, K. Jadhav, ournal of Alloys and Compounds, vol. 835, pp. 155422, 2020;

https://doi.org/10.1016/j.jallcom.2020.155422

[7] M. S. Kumar, G. Shankarmurthy, E. Melagiriyappa, K. Nagaraja, H. Jayanna, M. Telenkov, Journal of magnetism and Magnetic materials, vol. 478, pp. 12-19, 2019; https://doi.org/10.1016/j.jmmm.2019.01.058

[8] G. R. Amiri, M. Yousefi, M. Abolhassani, S. Manouchehri, M. Keshavarz, S. Fatahian, Journal of magnetism and magnetic materials, vol. 323, no. 6, pp. 730-734, 2011; https://doi.org/10.1016/j.jmmm.2010.10.034

[9] M. Mohapatra, S. Anand, International Journal of Engineering, Science and Technology, vol. 2, no. 8, 2010; https://doi.org/10.4314/ijest.v2i8.63846

[10] E. Manova, D. Paneva, B. Kunev, E. Rivière, C. Estournès, I. Mitov, "Characterization of nanodimensional Ni-Zn ferrite prepared by mechanochemical and thermal methods." p. 012102; https://doi.org/10.1088/1742-6596/217/1/012102

[11] B. T. Naughton, P. Majewski, D. R. Clarke, Journal of the American Ceramic Society, vol. 90, no. 11, pp. 3547-3553, 2007; https://doi.org/10.1111/j.1551-2916.2007.01981.x

[12] R. K. Singh, C. Upadhyay, S. Layek, A. Yadav, International Journal of Engineering, Science and Technology, vol. 2, no. 8, 2010; https://doi.org/10.4314/ijest.v2i8.63832

[13] K. Velmurugan, V. S. K. Venkatachalapathy, S. Sendhilnathan, Materials Research, vol. 13, pp. 299-303, 2010; https://doi.org/10.1590/S1516-14392010000300005

[14] A. Kumar, M. Arora, M. Yadav, R. Panta, Physics Procedia, vol. 9, pp. 20-23, 2010; https://doi.org/10.1016/j.phpro.2010.11.006

[15] L. Sonia, M. Victory, S. Phanjoubam, Integrated Ferroelectrics, vol. 204, no. 1, pp. 100-111, 2020; https://doi.org/10.1080/10584587.2019.1674978

[16] D. S. Mathew, R.-S. Juang, Chemical engineering journal, vol. 129, no. 1-3, pp. 51-65, 2007; https://doi.org/10.1016/j.cej.2006.11.001

[17] M. Sivakumar, T. Takami, H. Ikuta, A. Towata, K. Yasui, T. Tuziuti, T. Kozuka, D. Bhattacharya, Y. Iida, The Journal of Physical Chemistry B, vol. 110, no. 31, pp. 15234-15243, 2006; https://doi.org/10.1021/jp055024c

[18] U. Holzwarth, N. Gibson, Nature nanotechnology, vol. 6, no. 9, pp. 534-534, 2011; https://doi.org/10.1038/nnano.2011.145

[19] A. W. Burton, K. Ong, T. Rea, I. Y. Chan, Microporous and Mesoporous Materials, vol. 117, no. 1-2, pp. 75-90, 2009; https://doi.org/10.1016/j.micromeso.2008.06.010

[20] P. P.Sarangi, B.D.Naik,S.R. Vadera, M. K.Patra, C.Prakash, N.N .Ghosh, Materials Technology,vol. 24,no.2, PP.97-99, (2009); https://doi.org/10.1179/175355509X387156

[21] S. Ameer, I. H. Gul, N. Mahmood, M. Mujahid, Optical Materials, vol. 45, pp. 69-75, 2015; https://doi.org/10.1016/j.optmat.2015.02.035

[22] R. Ahmad, I. H. Gul, M. Zarrar, H. Anwar, M. B. Khan Niazi, A. Khan, Journal of magnetism and magnetic materials, vol. 405, pp. 28-35, 2016; https://doi.org/10.1016/j.jmmm.2015.12.019

[23] S. B. Khan, S. Irfan, S.-L. Lee, Nanomaterials, vol. 9, no. 7, pp. 1024, 2019; https://doi.org/10.3390/nano9071024

[24] M. Gabal, Journal of Magnetism and Magnetic Materials, vol. 321, no. 19, pp. 3144-3148, 2009; https://doi.org/10.1016/j.jmmm.2009.05.047

[25] M.Ahmed, S. Mansour , El-Dek SI, Solid State Ionics. 2010;181(25-26):1149-1555; https://doi.org/10.1016/j.ssi.2010.06.031

[26] A. Mohammad, M. Mohammed, and L. Hussein, Digest Journal of Nanomaterials and Biostructures, vol. 15, no. 1, pp. 231-241, 2020.

[27] S. Patil, V. Mahajan, A. Ghatage, S. Lotke, Materials chemistry and physics, vol. 57, no. 1, pp. 86-91, 1998; https://doi.org/10.1016/S0254-0584(98)00202-8

[28] A. M. Mohammad, S. M. A. Ridha, T. H. Mubarak, Int. J. Appl. Eng. Res, vol. 13, no. 8, pp. 6026-6035, 2018.

[29] S. Calvin, E. Carpenter, B. Ravel, V. Harris, S. Morrison, Physical Review B, vol. 66, no. 22, pp. 224405, 2002; https://doi.org/10.1103/PhysRevB.66.224405

748

[30] D. Fatemi, V. Harris, V. Browning, J. Kirkland, Journal of Applied Physics, vol. 83, no. 11, pp. 6867-6869, 1998; https://doi.org/10.1063/1.367766

[31] S.Lashkenari, M. Ghorbani, M.Naghibi, P. Khalaj," Polymer-Plastics Technology and Materials, vol.58,no.13, pp.1461-1470,2019; https://doi.org/10.1080/25740881.2018.1563124